



HAL
open science

Operating Frequency Range of Air Core Magnetic Inductors for Very High Frequency Power Converters

Florentin Salomez, Ansley Jugoo, Yves Lembeye

► **To cite this version:**

Florentin Salomez, Ansley Jugoo, Yves Lembeye. Operating Frequency Range of Air Core Magnetic Inductors for Very High Frequency Power Converters. 2024 IEEE Design Methodologies Conference (DMC 2024), Nov 2024, Grenoble, France. 10.1109/DMC62632.2024.10812116 . hal-04913092

HAL Id: hal-04913092

<https://hal.science/hal-04913092v1>

Submitted on 27 Jan 2025


HAL is a multi-disciplinary open access archive for the deposit and dissemination of scientific research documents, whether they are published or not. The documents may come from teaching and research institutions in France or abroad, or from public or private research centers.

L'archive ouverte pluridisciplinaire **HAL**, est destinée au dépôt et à la diffusion de documents scientifiques de niveau recherche, publiés ou non, émanant des établissements d'enseignement et de recherche français ou étrangers, des laboratoires publics ou privés.




Distributed under a Creative Commons Attribution - NonCommercial - ShareAlike 4.0 International License

Operating frequency range of air core magnetic inductors for very high frequency power converters

Florentin Salomez 
 Univ. Grenoble Alpes, CNRS,
 Grenoble INP*, G2ELab
 38000 Grenoble, France
 florentin.salomez@grenoble-inp.fr

Ansley Jugoo
 Univ. Grenoble Alpes, CNRS,
 Grenoble INP*, G2ELab
 38000 Grenoble, France
 ansley.jugoo@grenoble-inp.fr

Yves Lembeye 
 Univ. Grenoble Alpes, CNRS,
 Grenoble INP*, G2ELab
 38000 Grenoble, France
 yves.lembeye@grenoble-inp.fr

Abstract—The wide band gap transistors allow high or very high frequency operation of power converters. But the losses due to the magnetic materials increase a lot at these frequencies. Designers might consider not using magnetic materials at all. This paper addresses the question of the frequency range at which air core inductors will have a lower volume than counterparts with magnetic material for a given quality factor.

Index Terms—DC-DC power converters, inductors, design methodology, magnetic materials.

I. INTRODUCTION

The advance of wide band gap (WBG) transistors like Gallium Nitride (GaN) and Silicon Carbide (SiC) ones have allowed high frequency (HF) operation of power converters. But at the same time the magnetic materials used in power converters have not evolved much. The HF operation of magnetic component made of ferrite causes high losses. Without a breakthrough in material science, the designer of power converters should decide whether to use them or not at HF and Very High Frequency (VHF) [1], [2]. In this paper the frequency range where air core magnetic components outperform ferrite ones is studied for a given quality factor. The higher the quality factor, the better the converter's overall efficiency [3]–[5]. The approach considers the losses and a simple thermal model of magnetic components sized for resonant operation in a resonant VHF power converter (hypothesis of a pure sinewave current as excitation and constant reactance over the frequency range studied). A magnetic materials survey for VHF application is detailed in the section II. The section III presents the design problem under the formalism of optimization. Then section IV shows the thermal and losses models used in the optimization. The results are discussed in section V. Finally, section VI concludes this paper and gives some perspectives.

II. MAGNETIC MATERIALS SURVEY FOR VHF BAND

The goal of this section is to identify candidate magnetic materials for the VHF band and then to model them for optimization purpose. First, a quick survey based on the small

This work is supported by the French National Research Agency in the framework of the "Investissements d'avenir" program (ANR-15-IDEX-02), via the project CDP PowerAlps.

*Institute of Engineering Univ. Grenoble Alpes

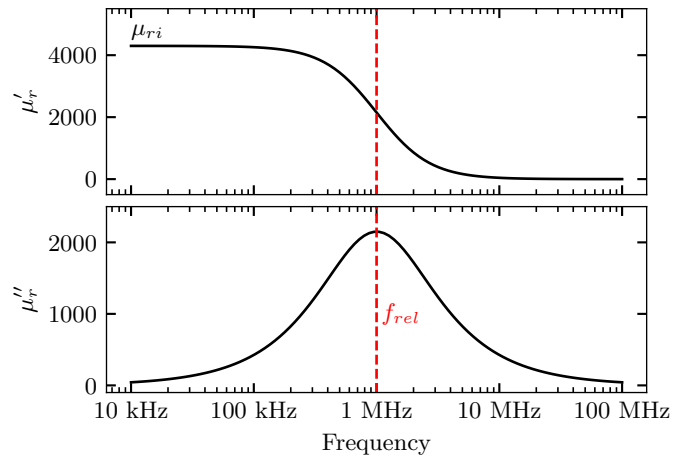


Fig. 1. Theoretical complex relative permeability spectrum of N30 Mn-Zn material built with Debye model.

signal response of the materials is performed. The data are extracted from the manufacturers' data-sheets. Second the data availability regarding the losses is studied. Finally the losses of one selected material are behaviourally modelled.

A. Frequency Behaviour

The frequency behaviour of the ferrite magnetic materials in small signals is well-know [6], [7]. As shown in the complex permeability spectrum in the Fig. 1, the primary permeability decreases from the initial one μ_{ri} to 1. The decrease of magnetic permeability with frequency is due in part to gyromagnetic resonance in the material [8]. The losses, represented by μ''_r are at maximum at the relaxation frequency f_{rel} . This behaviour can be modelled with a Debye like model [9] of the complex magnetic permeability

$$\mu_r(f) = \left(\frac{1}{\mu_{ri}} - \frac{f}{j \cdot (\mu_{ri} - 1) \cdot f_{rel}} \right)^{-1} \quad (1)$$

with j the unit imaginary number. This model allows to describe the first order relaxation in the magnetic permeability spectrum of whatever ferrite with only two parameters: μ_{ri} and f_{rel} . The low frequency losses due to hysteresis are not represented by this model. The Fig. 2 shows the relationship

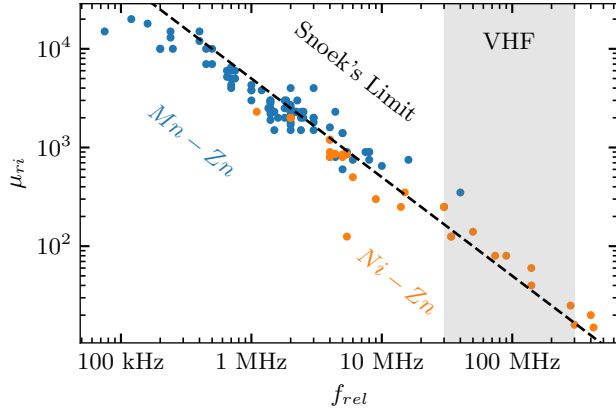


Fig. 2. Evolution of the initial relative permeability as a function of the relaxation frequency of different ferrites from two families Mn-Zn and Ni-Zn.

between the two parameters. As illustrated by the black dotted line, the majority of the considered ferrites follows a limit, called Snoek's limit [10]. This limit is defined as

$$S = (\mu_{ri} - 1) \cdot 2\pi f_{rel}. \quad (2)$$

It shows that the higher the frequency range of the ferrite, the lower its initial permeability. This means that for VHF application, only low permeability Ni-Zn material are considered.

B. Data Availability

Among the Ni-Zn materials a subset of them have been retained for this article and presented in the Table I. Since the goal here is to study the operating frequency range of these materials in comparison to air, the Table I focuses on the availability of losses data. Usually, losses data (for a sinusoidal excitation) are presented as volumetric losses P_V as a function of the temperature T for different couples of maximal magnetic induction and frequency (B_{max}, f) or as P_V as a function of B_{max} for different couples of (f, T). It's also possible to model the losses thanks to a Steinmetz frequency dependent model as performed in [1]. As shown in the Table I, the data is not always available in the datasheets from the suppliers and the temperature dependence of the losses is not always captured by the conventional Steinmetz model. The most complete dataset is for the material 67 from *Fair-Rite*. For other materials like the 4F1 from *Ferroxcube* only the charts in the datasheet are available which leads to extraction of data thanks to tools like [11]–[13].

It should be noted that for Mn-Zn materials much more data (with other excitation than sinusoidal) are available thanks to initiatives like MagNet [14], [15]. This database and standard to evaluate the losses of magnetic materials might be interesting to apply to Ni-Zn ferrites for HF and VHF applications.

III. DESIGN PROBLEM

A ring core inductor, as presented in Fig. 3 (a), is considered for this study. The internal radius is r , external radius R and

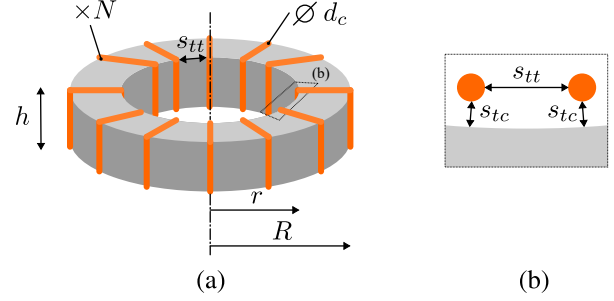


Fig. 3. Drawings of the ring core: (a) overview and (b) close-up on a pair of turns on the inner diameter.

height h . The single-layer (SL) winding is made of N turns of copper wire of diameter d_c and is spaced from the core by a distance s_{tc} . Two consecutive turns are spaced on the inner perimeter by a distance s_{tt} as shown in the Fig. 3 (b). Its inductance L is assumed frequency independent and its equivalent series resistance R_s is frequency dependent and is directly related to the total losses P_{tot} (which are the sum of the copper winding losses P_{Cu} and core losses P_{iron}) such that $P_{tot} = R_s(f) \cdot I_{RMS}^2$. The inductor is designed with the objective of minimizing its external wounded volume

$$V_{ext} = \pi \cdot (R + d_c + s_{tc})^2 \cdot (h + 2 \cdot (d_c + s_{tc})), \quad (3)$$

such that the reactance X_L at the frequency f is equal to the requirement, with a lower bound for the quality factor $Q = X_L/R_s$ expressed as the maximal losses allowed P_{max} . The maximum temperature is fixed at $T_{max} = 90^\circ C$ and only one layer of winding with a fraction coverage of $k_{SL} = 0.9$ is allowed in order to keep the parasitic capacitance low. For the case where a magnetic material is used, the constraint of the Non Saturation (NS) of the core on the internal perimeter is added with H_{max} the maximum magnetic field excitation allowed. The degrees of freedom are the internal radius of the core r , the number of turns N and the wire diameter d_c . The external radius and height are deduced from the internal radius by fixed form factors $R = k_R \cdot r = \exp(1/2) \cdot r$ and $h = k_h \cdot R = 0.9 \cdot \exp(1/2) \cdot r$ (fitted on available commercial ring core dimensions). This problem is expressed as an optimization problem hereafter:

$$\min_{(r, d_c, N)} V_{ext} \quad (\text{enclosed volume}), \quad (4)$$

subject to

$$P_{tot}(T) < P_{max} \quad (\text{losses}), \quad (5a)$$

$$T < T_{max} \quad (\text{temperature}), \quad (5b)$$

$$L = \mu_0 \mu_{ri} \cdot \frac{k_h \cdot r}{4\pi} \quad (\text{inductance}), \quad (5c)$$

$$N < N_{max} \quad (\text{SL}), \quad (5d)$$

$$\frac{N \cdot I_{max}}{2\pi r} < H_{max} \quad (\text{NS}), \quad (5e)$$

with the total losses

$$P_{tot}(T) = P_{iron}(T) + P_{Cu}, \quad (6)$$

TABLE I
NI-ZN MATERIALS SURVEY FOR THE VHF BAND AND DATA AVAILABILITY (SEPT. 2024).

Material	μ_{ri}	f_{rel} (MHz)	$P_V = f(T)$	$P_V = f(B_{max})$	Steinmetz Coefficients
Ferroxcube 4F1	80	90	chart in [16] 3 $\leq f \leq$ 10 MHz 7.5 $\leq B_{max} \leq$ 10 mT 0 $\leq T \leq$ 120 °C	chart in [16] 3 $\leq f \leq$ 10 MHz 3 $\leq B_{max} \leq$ 30 mT $T =$ 100 °C	table in [1] 2 $\leq f \leq$ 20 MHz $T =$? °C
Fair-Rite 52	250	14	no data in [17]	no data in [17]	table in [1] 2 $\leq f \leq$ 7 MHz $T =$? °C
Fair-Rite 61	125	34	chart in [18] 2 $\leq f \leq$ 15 MHz 5 $\leq B_{max} \leq$ 20 mT 20 $\leq T \leq$ 120 °C	chart in [18] 2 $\leq f \leq$ 15 MHz 1.5 $\leq B_{max} \leq$ 30 mT $T =$ 25 °C	table in [1] 2 $\leq f \leq$ 16 MHz $T =$? °C
Fair-Rite 67	40	140	chart and .csv in [19] 2 $\leq f \leq$ 20 MHz 5 $\leq B_{max} \leq$ 20 mT 10 $\leq T \leq$ 120 °C	charts and .csv in [19] 2 $\leq f \leq$ 20 MHz 2 $\leq B_{max} \leq$ 26 mT $T \in \{25, 100\}$ °C	table in [1] 2 $\leq f \leq$ 60 MHz $T =$? °C
Fair-Rite 68	250	300	no data in [20]	no data in [20]	table in [1] 10 $\leq f \leq$ 20 MHz $T =$? °C

The maximal power losses allowed is

$$P_{max} = \frac{X_L}{Q} I_{RMS}^2 = \frac{2\pi f L}{Q} I_{RMS}^2. \quad (7)$$

The maximum number of turns on a single layer winding is

$$N_{max} = \frac{2\pi \cdot k_{SL,max} \cdot (r - \frac{d_c}{2} - s_{tc})}{d_c + s_{tt}}. \quad (8)$$

IV. THERMAL AND LOSSES MODELS

The total losses for the air core are solely due to winding losses (equivalent to $P_{iron} = 0$) whereas the core losses are also considered for the ferrite core.

A. Winding Losses

The winding losses P_{Cu} are modelled with the Dowell approach [6] by considering a single layer winding and temperature independence. The equivalent AC resistance is defined as $R_{AC} = F \cdot R_{DC}$ with the Dowell factor

$$F = \Re(\alpha \cdot c \cdot \coth(\alpha \cdot c)). \quad (9)$$

The Dowell factor is computed for an equivalent square cross-section conductor of same surface area than the round conductor used here, such that its side is

$$c = \sqrt{\frac{\pi}{4} \cdot d_c}. \quad (10)$$

The parameter α is defined as

$$\alpha = \sqrt{j \frac{2\pi f \mu_0 \eta}{\rho_{Cu}}}, \quad (11)$$

with

$$\eta = \frac{c}{s_{tt} + d_c}, \quad (12)$$

and ρ_{Cu} the resistivity of copper. It should be noted that more precise models dedicated to ring core windings exist and are presented in [21]. The application of such models will be studied in subsequent work.

B. Magnetic losses behavioural modelling

The requirements for the design by optimization used in this article depend upon the chosen solver. The solver considered in this work is a Sequential Least Squares Programming (SLSQP) algorithm from the SciPy 1.9.1 module [22], [23] for Python. This algorithm has been chosen in particular because it is among the few in the `scipy.minimize` module to enforce non linear constraints [22, Table 1]. The use of this specific algorithm implies the following requirements on the models used hereafter:

- continuous models,
- models at least once derivable.

These requirements make possible the use of interpolation models like cubic splines, but the datasets used here are quite small. For example there are only 15 couples of (B_{max}, f) with each 4 temperature points for the volumetric losses as a function of temperature for the *Fair-Rite 67* material (60 data points). This seriously restrains the evaluation space used by the solver. To ensure extrapolation and evaluation of the losses outside of the original dataset, physical models of magnetic losses based on hysteresis cycles are available, like Jiles Atherton models [24] or eddy current models like in [25]–[27]. It is also possible to use behavioural models like the Steinmetz model [28] and its derivatives [29]–[31] for non sinusoidal excitation or for temperature dependence [32]. Here a behavioural model from ferrite manufacturer [33], [34] is chosen for its simplicity of use and temperature dependence.

TABLE II
FITTED TEMPERATURE DEPENDENT STEINMETZ PARAMETERS FOR THE
MATERIAL FAIR-RITE 67.

Material	α	β	C_{T2}	C_{T1}	C_{T0}
FR67	1.11	2.02	$2.86 \cdot 10^{-3}$	$-1.08 \cdot 10^{-1}$	$3.73 \cdot 10^1$

The volumetric losses are expressed with a temperature dependent Steinmetz model as

$$P_V(f, T, B_{max}) = f^\alpha \cdot B_{max}^\beta \cdot (C_{T2} \cdot T^2 - C_{T1} \cdot T + C_{T0}), \quad (13)$$

with $\alpha, \beta, C_{T0}, C_{T1}, C_{T2}$ fitted constants.

This model has been fitted on the supplier's data for the material *Fair-Rite* 67. The results are shown in the Fig. 4 and in Table II. The order of magnitude is correctly reproduced by the model, but more degrees of freedom would be required to improve the fitting, especially to take into account the joint effect of temperature and frequency (at low frequency the temperature dependence is not the same than that of high frequency). Here the relative error of the model to the data is smaller for the high frequency part. Since our study is focused on the VHF band, the model is kept as it is afterwards.

Then the iron losses are computed by

$$P_{iron}(T, f, B_{max}) = P_V(f, T, B_{max}) \cdot V_{iron}, \quad (14)$$

with

$$V_{iron} = \pi \cdot (R^2 - r^2) \cdot h = \pi \cdot (k_R - 1) \cdot k_h \cdot k_R \cdot r^3 \quad (15)$$

C. Thermal Model

The thermal model is common for both the air core inductor and the ferrite one. The thermal model is based upon empirical relation [8], [9], [10] that describes the temperature rise ΔT as a function of the total losses P_{tot} in mW and the overall external surface of the wound core S_{ext} in cm^2 such that

$$\Delta T = \left(\frac{P_{tot}(T) \cdot 10^3}{S_{ext} \cdot 10^4} \right)^{0.833}. \quad (16)$$

For ferrite core P_{tot} is dependent upon $T = T_a + \Delta T$ with T_a the ambient temperature, as shown previously. So ΔT is computed iteratively until it converges to an equilibrium temperature or that it goes over a preset runaway temperature (here $T_{runaway} = 120^\circ\text{C}$). The external surface is defined as

$$S_{ext} = k_{SL} \cdot S_{wind} + (1 - k_{SL}) \cdot S_{core}, \quad (17)$$

with S_{wind} the external surface of the ring core that includes the winding such that

$$S_{wind} = \pi \cdot ((R + d_c + s_{tc})^2 - (r + d_c + s_{tc})^2) + 2\pi \cdot (R + r) \cdot (h + 2 \cdot (d_c + s_{tc})), \quad (18)$$

with k_{SL} the winding coverage fraction such that

$$k_{SL} = \frac{N \cdot (s_{tt} + d_c)}{2\pi \cdot (r - \frac{d_c}{2} - s_{tc})} \quad (19)$$

and S_{core} the external surface of the core such that

$$S_{core} = \pi \cdot (R^2 - r^2) + 2\pi \cdot (R + r) \cdot h. \quad (20)$$

For air core inductor the winding is held by a plastic core so S_{core} is discarded.

V. RESULTS AND DISCUSSION

The optimization problem presented previously is applied on a range of frequencies from 50 kHz to 300 MHz and on a range of minimal Q from 50 to 200. These applications are repeated for air core and Ni-Zn core inductors. The results of the optimization are shown for air core inductors in Fig. 5 and for Ni-Zn core inductors in Fig. 6.

A. Analysis for air core inductors

The results presented in Fig. 5 shows that the optimal volume of the inductor decreases with the frequency for all the Q factor evaluated. According to the P_{tot} axis the volume is constrained primarily by the maximum losses allowed. Then for increasing frequencies the maximum temperature constraint is reached and the decreasing slope of volume is less steep than in low frequency. It is mainly due to the internal radius that reaches the lower bound. The non-respect of the minimal bound for the internal radius might be due to the automatic differentiation used in the algorithm that does not respect the bounds, especially on the edge [35]. Therefore, in subsequent work, the jacobian matrix of the problem will be computed beforehand to avoid automatic differentiation.

The minimum Q reachable is capped by the upper bound on the conductor diameter. Indeed for air core inductor the only way to reduce losses is to increase the conductor diameter and to reduce its length.

B. Analysis for NiZn inductors

The results presented in Fig. 6 shows that the optimal volume of the inductor increases with frequency for all the Q factor evaluated. According to the temperature T axis the volume is first constrained by maximum temperature in low frequency, then for higher frequency the maximum allowable losses are reached. The upper bound of the conductor diameter is reached at low frequency (100 kHz), this limit the frequency range for a given Q factor. Indeed, as the frequency increases the core losses increase also and the only way to reduce them is to enlarge the volume and the conductor diameter until the core is too large to achieve the required inductance.

The non continuity of the solution might be due to bad conditioning of the numerical problem and some numerical noise in the evaluation of the final temperature of the core. This will be refined in subsequent work.

C. Comparison between air core and NiZn core inductors

First, the overall trend is mostly the opposite of one another. For air core inductors higher Q are achievable at higher frequencies (> 10 MHz) and for Ni-Zn core inductors higher Q are achievable at lower frequencies (< 1 MHz).

Second, for low Q like 50, $X_L = 50 \Omega$ and $I_{max} = 1$ A air core achieves a lower volume than Ni-Zn core for frequencies roughly higher than 300 kHz. This trend is also confirmed for higher Q but at higher frequencies. This confirms the trends

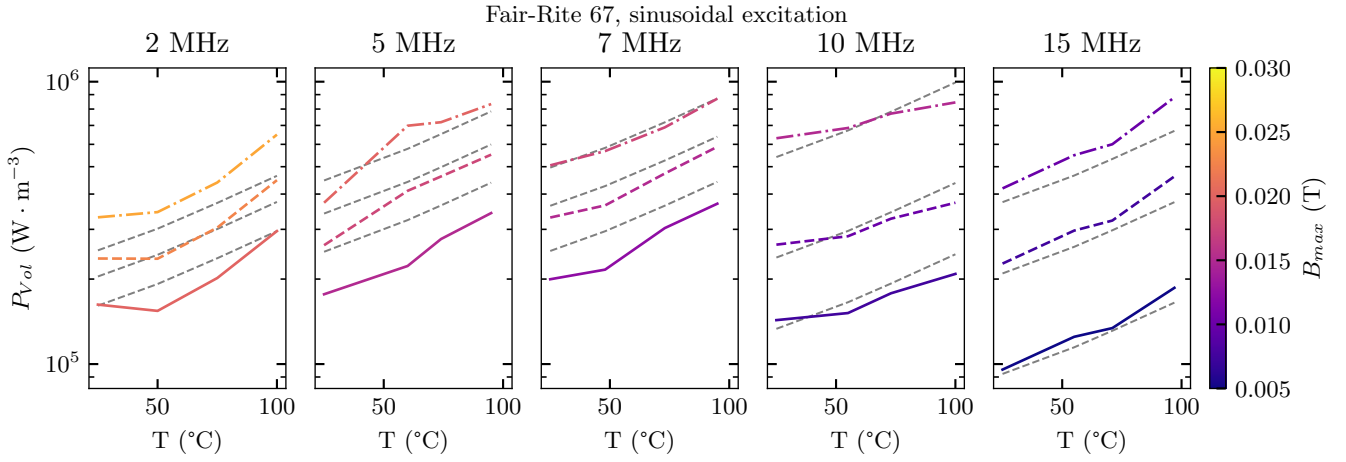


Fig. 4. Volumetric losses of Fair-Rite 67 ferrite material as a function of the temperature T , the peak magnetic induction B_{max} , the frequency f . The model is plotted for each available value in grey dashed line.

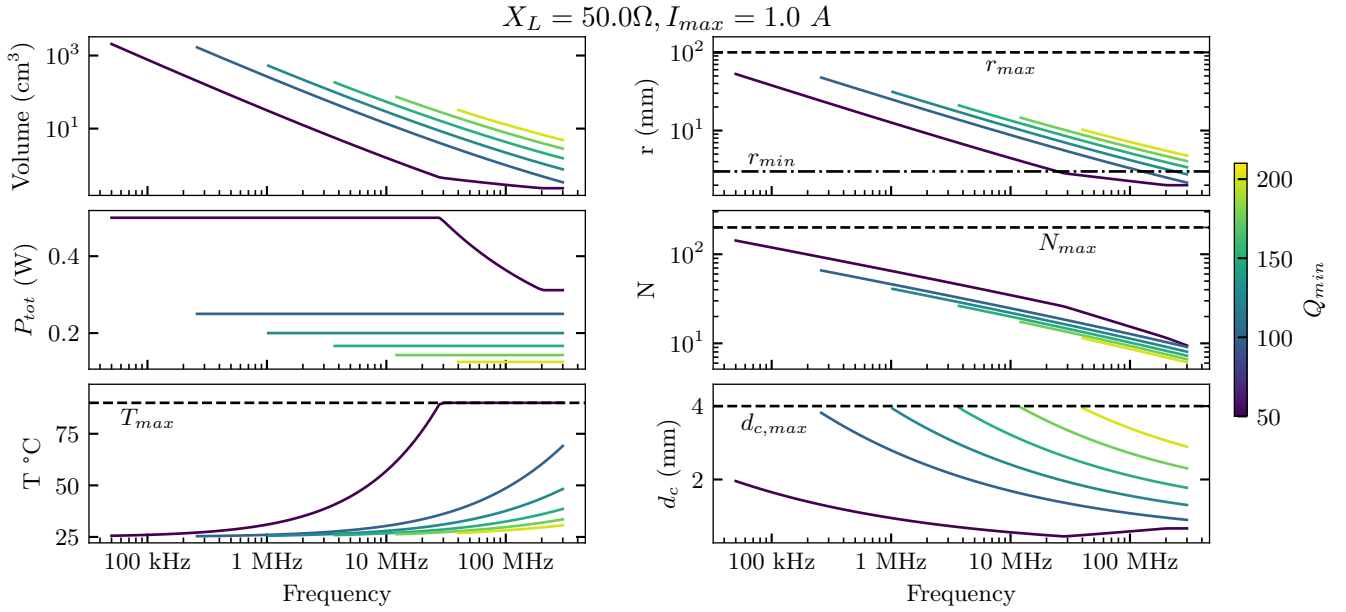


Fig. 5. Optimization results for the air core inductors: the left column shows the objective function and some of the constraints, the right column shows the value of the degrees of freedom after optimization. The remaining parameters are $s_{tc} = 0.1$ mm, $s_{tt} = 0.1$ mm, $\beta = 0.9$. The non continuity of the solution might be due to bad conditioning of the numerical problem and some numerical noise in the evaluation of the final temperature of the core

observed in the results shown in [1], [2]. But it shows also that, depending the requirements, air core might outperform cored inductors even in a lower frequency band than observed in the literature (5 to 50 MHz).

Third, for a frequency range between 150 kHz and 20 MHz and a Q of more than 175 there are no solutions (among the two options considered here: air and one Ni-Zn) for the considered requirements. This point is really important and should be studied in the future to understand whether these ranges are reachable with other magnetic materials or not. This analysis might help future designers to choose their magnetic material and help also magnetic material manufacturers to identify new operational range to reach.

Finally, this work lack experimental validation. This is part

of subsequent work on the subject.

VI. CONCLUSIONS AND PERSPECTIVES

The operating frequency range of air core magnetic inductors with a minimum volume and for sine-wave resonant power converters depends mainly on the wanted Q factor and the requirements of the application.

This article shows that for lower Q , the air core inductors are serious contender to Ni-Zn cores in terms of volume. For frequencies higher than 10 MHz, the air core inductor is always smaller in volume in comparison to Ni-Zn one for the considered requirements. It shows also that the higher the frequency the higher the Q of the air core and the opposite for Ni-Zn ones.

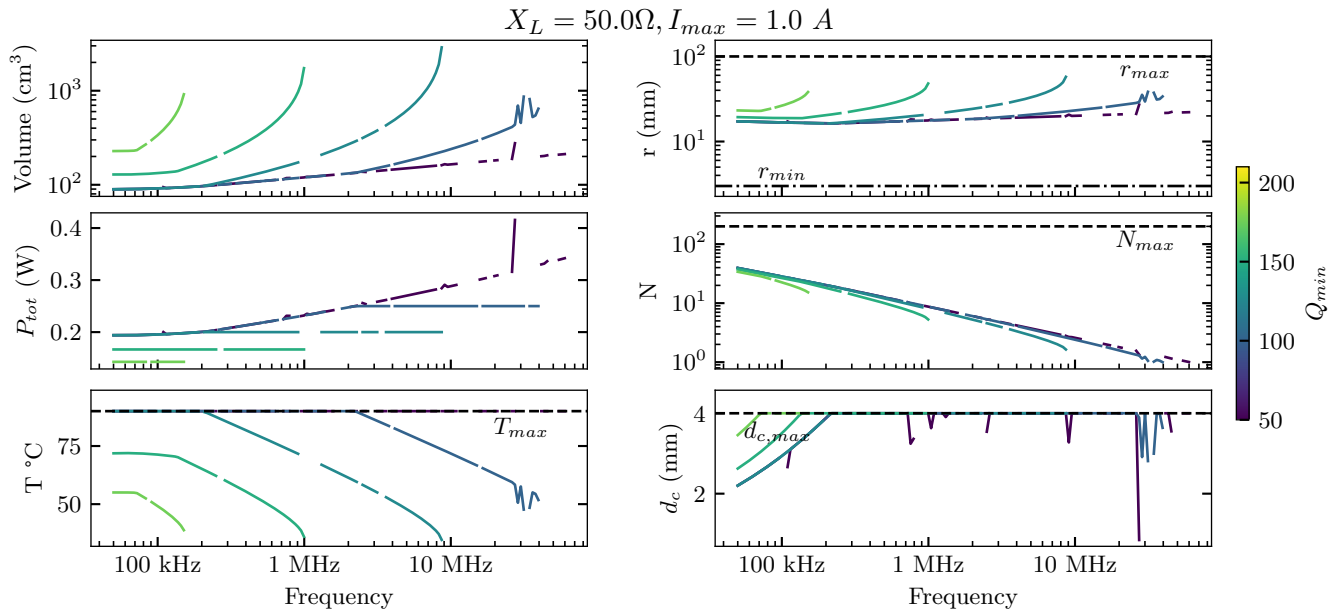


Fig. 6. Optimization results for the Ni-Zn core inductors: the left column shows the objective function and some of the constraints, the right column shows the value of the degrees of freedom after optimization. The remaining parameters are $s_{tc} = 0.1$ mm, $s_{tt} = 0.1$ mm, $\beta = 0.9$.

The prospects for this work are multiple. First the survey of magnetic materials for VHF application have shown that data about the magnetic losses are scarce. A campaign of measurements is required to characterize the losses among the Ni-Zn materials with temperature dependence and for several excitation waveforms. These data will greatly help any designer to size correctly its magnetic components. In addition, it will also help to answer more precisely the question presented in this article. Therefore these data should be encoded in an open data format and freely available to the community (like the initiative from MagNet for example). Second the magnetic losses models with temperature dependence and the thermal models need to be refined to accurately evaluate the losses and temperature of cores for whatever combination of frequency, peak induction, temperature and waveforms. Finally, thanks to the two previous points, it will be possible to study in deep the operating frequency range of several magnetic materials in comparison to air and to validate the findings thanks to experimental work.

REFERENCES

- [1] A. J. Hanson, J. A. Belk, S. Lim, C. R. Sullivan, and D. J. Perreault, "Measurements and performance factor comparisons of magnetic materials at high frequency," *IEEE Transactions on Power Electronics*, vol. 31, no. 11, pp. 7909–7925, 2016. doi: 10.1109/TPEL.2015.2514084
- [2] M. Solomentsev and A. J. Hanson, "At What Frequencies Should Air-Core Magnetics Be Used?" *IEEE Transactions on Power Electronics*, vol. 38, pp. 3546–3558, Mar. 2023. doi: 10.1109/TPEL.2022.3222993 Conference Name: IEEE Transactions on Power Electronics.
- [3] D. J. Perreault, J. Hu, J. M. Rivas, Y. Han, O. Leitermann, R. C. Pilawa-Podgurski, A. Sagneri, and C. R. Sullivan, "Opportunities and Challenges in Very High Frequency Power Conversion," in *2009 Twenty-Fourth Annual IEEE Applied Power Electronics Conference and Exposition*, Feb. 2009. doi: 10.1109/APEC.2009.4802625 pp. 1–14, ISSN: 1048-2334.
- [4] A. Knott, T. M. Andersen, P. Kamby, J. A. Pedersen, M. P. Madsen, M. Kovacevic, and M. A. E. Andersen, "Evolution of Very High Frequency Power Supplies," *IEEE Journal of Emerging and Selected Topics in Power Electronics*, vol. 2, no. 3, pp. 386–394, Sep. 2014. doi: 10.1109/JESTPE.2013.2294798. [Online]. Available: <http://ieeexplore.ieee.org/document/6680598/>
- [5] Y. Wang, O. Lucia, Z. Zhang, Y. Guan, and D. Xu, "Review of very high frequency power converters and related technologies," *IET Power Electronics*, vol. 13, no. 9, pp. 1711–1721, 2020. doi: <https://doi.org/10.1049/iet-pel.2019.1301>. [Online]. Available: <https://ietresearch.onlinelibrary.wiley.com/doi/abs/10.1049/iet-pel.2019.1301>
- [6] J. Smit and H. P. Wijn, *FERRITES - PHYSICAL PROPERTIES AND TECHNICAL APPLICATIONS - by J.SMIT and H.P.J.WIJN*, 1959. [Online]. Available: <http://archive.org/details/PHILIPS1959SmitWijnFerrites>
- [7] E. C. E. C. Snelling, *Soft ferrites: properties and applications*. Cleveland, Ohio, CRC Press, 1969. [Online]. Available: <http://archive.org/details/softferritesprop0000snel>
- [8] J. L. Snoek, "Gyromagnetic Resonance in Ferrites," *Nature*, vol. 160, no. 4055, pp. 90–90, Jul. 1947. doi: 10.1038/160090a0 Publisher: Nature Publishing Group. [Online]. Available: <https://www.nature.com/articles/160090a0>
- [9] N. Hamilton, "Electrical circuit models of the hf initial permeability spectra of soft ferrite lead to revised definition of fundamental material properties," in *1st Annual Active and Passive RF Devices Seminar*, 2013. doi: 10.1049/ic.2013.0239 pp. 59–62.
- [10] J. L. Snoek, "Dispersion and absorption in magnetic ferrites at frequencies above one Mc/s," *Physica*, vol. 14, no. 4, pp. 207–217, May 1948. doi: 10.1016/0031-8914(48)90038-X. [Online]. Available: <https://www.sciencedirect.com/science/article/pii/003189144890038X>
- [11] "automeris.io: Computer vision assisted data extraction from charts using WebPlotDigitizer." [Online]. Available: <https://automeris.io/>
- [12] "Engauge Digitizer." [Online]. Available: <https://markumitchell.github.io/engauge-digitizer/>
- [13] P. Novak, "g3data." Jun. 2024, original-date: 2010-12-01T04:18:58Z. [Online]. Available: <https://github.com/pn2200/g3data>
- [14] H. Li, D. Serrano, T. Guillod, E. Dogariu, A. Nadler, S. Wang, M. Luo, V. Bansal, Y. Chen, C. R. Sullivan, and M. Chen, "MagNet: An Open-Source Database for Data-Driven Magnetic Core Loss Modeling," in *2022 IEEE Applied Power Electronics Conference and Exposition (APEC)*, Mar. 2022. doi: 10.1109/APEC43599.2022.9773372 pp. 588–595, ISSN: 2470-6647.
- [15] "MagNet." [Online]. Available: <https://mag-net.princeton.edu/>

- [16] Ferroxcube, "Datasheet 4F1." [Online]. Available: <https://ferroxcube.home.pl/prod/assets/4f1.pdf>
- [17] Fair-Rite, "52 Material Data Sheet." [Online]. Available: <https://fair-rite.com/52-material-data-sheet/>
- [18] —, "61 Material™ Data Sheet." [Online]. Available: <https://fair-rite.com/61-material-data-sheet/>
- [19] —, "67 Material Data Sheet." [Online]. Available: <https://fair-rite.com/67-material-data-sheet/>
- [20] —, "68 Material Data Sheet." [Online]. Available: <https://fair-rite.com/68-material-data-sheet/>
- [21] G. Lefevre, H. Chazal, J. Ferrieux, and J. Roudet, "Application of dovwell method for nanocrystalline toroid high frequency transformers," in *2004 IEEE 35th Annual Power Electronics Specialists Conference (IEEE Cat. No.04CH37551)*, vol. 2, 2004. doi: 10.1109/PESC.2004.1355538 pp. 899–904 Vol.2.
- [22] P. Virtanen, R. Gommers, T. E. Oliphant, M. Haberland, T. Reddy, D. Cournapeau, E. Burovski, P. Peterson, W. Weckesser, J. Bright, S. J. van der Walt, M. Brett, J. Wilson, K. J. Millman, N. Mayorov, A. R. J. Nelson, E. Jones, R. Kern, E. Larson, C. J. Carey, Í. Polat, Y. Feng, E. W. Moore, J. VanderPlas, D. Laxalde, J. Perktold, R. Cimrman, I. Henriksen, E. A. Quintero, C. R. Harris, A. M. Archibald, A. H. Ribeiro, F. Pedregosa, P. van Mulbregt, and SciPy 1.0 Contributors, "SciPy 1.0: Fundamental Algorithms for Scientific Computing in Python," *Nature Methods*, vol. 17, pp. 261–272, 2020. doi: 10.1038/s41592-019-0686-2
- [23] "SciPy." [Online]. Available: <https://scipy.org/>
- [24] J. Izydorczyk, "Extraction of Jiles and Atherton parameters of ferrite from initial magnetization curves," *Journal of Magnetism and Magnetic Materials*, vol. 302, no. 2, pp. 517–528, Jul. 2006. doi: 10.1016/j.jmmm.2005.10.013
- [25] C. Beatrice, O. Bottauscio, M. Chiampi, F. Fiorillo, and A. Manzin, "Magnetic loss analysis in Mn–Zn ferrite cores," *Journal of Magnetism and Magnetic Materials*, vol. 304, no. 2, pp. e743–e745, Sep. 2006. doi: 10.1016/j.jmmm.2006.02.209. [Online]. Available: <https://www.sciencedirect.com/science/article/pii/S0304885306005415>
- [26] F. Fiorillo, C. Beatrice, O. Bottauscio, and E. Carmi, "Eddy-Current Losses in Mn-Zn Ferrites," *IEEE Transactions on Magnetics*, vol. 50, no. 1, pp. 1–9, Jan. 2014. doi: 10.1109/TMAG.2013.2279878 Conference Name: IEEE Transactions on Magnetics.
- [27] S. Dobák, C. Beatrice, V. Tsakaloudi, and F. Fiorillo, "Magnetic Losses in Soft Ferrites," *Magnetochemistry*, vol. 8, no. 6, p. 60, Jun. 2022. doi: 10.3390/magnetochemistry8060060 Number: 6 Publisher: Multidisciplinary Digital Publishing Institute. [Online]. Available: <https://www.mdpi.com/2312-7481/8/6/60>
- [28] C. P. Steinmetz, "On the law of hysteresis," *Transactions of the American Institute of Electrical Engineers*, vol. IX, no. 1, pp. 1–64, 1892. doi: 10.1109/T-AIEE.1892.5570437
- [29] J. Reinert, A. Brockmeyer, and R. De Doncker, "Calculation of losses in ferro- and ferrimagnetic materials based on the modified steinmetz equation," *IEEE Transactions on Industry Applications*, vol. 37, no. 4, pp. 1055–1061, 2001. doi: 10.1109/28.936396
- [30] J. Li, T. Abdallah, and C. Sullivan, "Improved calculation of core loss with nonsinusoidal waveforms," in *Conference Record of the 2001 IEEE Industry Applications Conference. 36th IAS Annual Meeting (Cat. No.01CH37248)*, vol. 4, 2001. doi: 10.1109/IAS.2001.955931 pp. 2203–2210 vol.4.
- [31] K. Venkatachalam, C. Sullivan, T. Abdallah, and H. Tacca, "Accurate prediction of ferrite core loss with nonsinusoidal waveforms using only steinmetz parameters," in *2002 IEEE Workshop on Computers in Power Electronics, 2002. Proceedings.*, 2002. doi: 10.1109/CIPE.2002.1196712 pp. 36–41.
- [32] K. Detka and K. Górecki, "Modelling the power losses in the ferromagnetic materials," *Materials Science-Poland*, vol. 35, no. 2, pp. 398–404, Jul. 2017. doi: 10.1515/msp-2017-0050. [Online]. Available: <https://sciendo.com/article/10.1515/msp-2017-0050>
- [33] "Ferroxcube 3F36 Datasheet." [Online]. Available: <https://www.ferroxcube.com/en-global/download/download/99>
- [34] "FC Steinmetz Coefficient Spreadsheet." [Online]. Available: <https://www.ferroxcube.com/upload/media/design/FXCSteinmetzCoefficients.xls>
- [35] "scipy.optimize.minimize SLSQP leads to out of bounds solution · Issue #3056 · scipy/scipy." [Online]. Available: <https://github.com/scipy/scipy/issues/3056#issuecomment-204802021>